Energy level alignment of self-assembled linear chains of benzenediamine on Au(111) from first principles

Guo Li, Tonatiuh Rangel, Zhen-Fei Liu, Valentino R. Cooper, and Jeffrey B. Neaton

Energy Level Alignment of Self-Assembled Linear Chains of

Benzenediamine on Au(111) from First Principles

Guo Li,[1,2,3,*] Tonatiuh Rangel,[2,3] Zhen-Fei Liu,[2,3] Valentino R. Cooper,[4] and Jeffrey B. Neaton[2,3,5,†]

[1] *The Joint Center of Artificial Photosynthesis, Lawrence Berkeley National Laboratory, Berkeley, California 94720, USA*

[2] *Molecular Foundry, Lawrence Berkeley National Laboratory, Berkeley, California 94720, USA*

[3] *Department of Physics, University of California, Berkeley, California 94720, USA*

[4] *Materials Science and Technology Division, Oak Ridge National Laboratory, Oak Ridge, Tennessee 37831, USA*

[5] *Kavli Energy NanoSciences Institute at Berkeley, Berkeley, California 94720, USA*

Using density functional theory (DFT) with van der Waals functionals, we calculate the adsorption energetics and geometry of benzenediamine (BDA) molecules on Au(111) surfaces. Our results demonstrate that the reported self-assembled linear chain structure of BDA, stabilized via hydrogen bonds between amine groups, is energetically favored over previously-studied monomeric phases. Moreover, using a model, which includes nonlocal polarization effects from the substrate and the neighboring molecules and incorporates many-body perturbation theory calculations within the GW approximation, we obtain approximate self-energy corrections to the DFT highest occupied molecular orbital (HOMO) energy associated with BDA adsorbate phases. We find that, independent of coverage, the HOMO energy of the linear chain phase is lower relative to the Fermi energy than that of the monomer phase, and in good agreement with values measured with ultraviolet photoelectron spectroscopy and X-ray photoelectron spectroscopy.

PACS numbers: 68.43.Fg, 68.43.Hn, 73.20.Hb, 73.64.-b, 73.50.-c

* Electronic address: guoli@lbl.gov

† Electronic address: jbneaton@lbl.gov

There is continued interest in using organic molecules as components in electronic and optoelectronic devices. [1-4] As a consequence, electronic energy level alignment at interfaces between organic components (such as individual molecules) and inorganic electrodes, which are critical to charge flow within organic devices, have been the focus of significant recent fundamental work [5-13]. When a molecule is in contact with an electrode, its orbital energies are significantly altered relative to the gas-phase by several competing physical contributions. Notably, interface dipoles, resulting from induced charge redistribution upon binding, can shift the molecular orbital energies either collectively upward or downward relative to the electrode Fermi level; [5,8,9] substrate polarization, associated with the addition of an electron or hole to the molecular adsorbate and leading to a renormalization of its fundamental gap, will shift frontier orbital energies either toward or away from the Fermi level, respectively. [6,7] Since these effects are sensitive to the adsorption geometry of the molecule, identifying the energetically favorable geometries is clearly essential to accurate prediction and understanding of adsorbate electronic structure.

The benzenediamine (BDA)-Au(111) system has been well studied as a prototypical metal-organic interface [18-21]. Additionally, BDA has been a "fruit-fly" molecule for the study of single-molecule junction transport properties and energy level alignment, leading to significant progress in both experiment [14,15] and theory [7,16,17]. The highest occupied molecular orbital (HOMO) resonance energies of the adsorbed BDA molecules have been experimentally measured with ultraviolet photoelectron spectroscopy (UPS) and X-ray photoelectron spectroscopy (XPS). [18] *Ab initio* calculations of BDA monomers adsorbed on Au(111) at low coverage in hypothetical geometries have interpreted these experiments, with quantitative success. [13,18-20] However, recently scanning tunneling microscope (STM) experiments [21] have provided new information about the adsorption geometry, revealing the formation of self-assembled linear chains of BDA molecules on Au(111) and raising questions about the origin of this assembly and its effects on electronic structure (relative to the monomeric phase assumed in prior works).

In this work, we use density functional theory (DFT) calculations to calculate the adsorption energetics of the self-assembled linear chain structure of BDA molecules on Au(111) observed experimentally. We compare this newly-reported linear chain phase with that of isolated BDA monomers as a function of coverage, and we find that the linear chains are energetically more stable than isolated monomers at all coverages. Furthermore, using an approximate self-energy-corrected method, which includes nonlocal polarization effects from the substrate and neighboring molecules, as well as information from GW calculations, we calculate the HOMO energies of the linear chain phases relative to the Au Fermi level (E_F), and show that they are in excellent agreement with experiments.

The majority of our DFT calculations are performed with the VASP code [22-25] using the generalized gradient approximation of Perdew, Burke, and Ernzerhof (PBE) [26,27] and a van der Waals (vdW) density functional (vdW-DF2) [28-32]. Our VASP calculations use a plane-wave basis and projector augmented-wave (PAW) potentials [33,34], requiring plane-wave and augmentation-charge cutoffs of 400 eV and 644.9 eV, respectively. To model Au(111) surfaces, we use supercells containing a four-atomic-layer slab and a 20 Å vacuum layer. We use the PBE functional to determine the Au lattice constant, and obtain 4.17 Å, consistent with prior calculations [35]. Our calculations of gas-phase BDA are performed with vdW-DF2 in a 20Å×20Å×20Å supercell with a single k point (Γ). For calculations of the self-assembled linear chains, we construct a surface with in-plane lattice parameters $\boldsymbol{a_1}' = 4\boldsymbol{a_1}+3\boldsymbol{a_2}$ and $\boldsymbol{a_2}'=2\boldsymbol{a_1}+\boldsymbol{a_2}$, where $\boldsymbol{a_1}$ and $\boldsymbol{a_2}$ are the primitive lattice vectors of Au(111) as indicated in Fig. 1. The corresponding surface area A is 0.75 nm^2, consistent with experiment. [21] BDA molecules have been reported to assemble into linear chains at an angle of 12° with the [112] direction [21], where the chains are separated from each other by about 1 nm. These linear structures, as well as those with larger separations, are also calculated with vdW-DF2 to determine coverage effects on the adsorption energetics and geometry; the details of our calculations are summarized in Table

3

S1 in the Supplemental Material (SM) [36]. For comparison, BDA monomers at different coverages are computed by centering a single BDA molecule on a $na_1 \times na_2$ Au(111) surface, where n is an integer in the range from 3 to 9, and optimizing the adsorbate geometry with vdW-DF2. In all calculations, the Au atoms are fixed in their bulk positions, and the molecules are fully relaxed until the forces on each atom are less than 0.01 eV/Å. In addition, dipole corrections [37,38] are used to remove spurious effects of the periodic boundary conditions. For different BDA phases in the absence of Au substrates (see additional details below), G_0W_0 calculations are performed with BerkeleyGW [39] from a DFT-PBE starting point [40] with the ABINIT package [41]. Technical details of our GW calculations are in the SM [36].

In Fig. 1a), we show the most stable configuration of an isolated adsorbed BDA molecule on a $4a_1 \times 4a_2$ slab. The BDA molecule is calculated to bind in the *trans*-conformation, consistent with prior results [21,42], and the long axis of the molecule is oriented along the [112] direction of the Au substrate. One of the BDA amine groups binds preferentially to a surface Au atom via a weak N-Au bond with a length of 2.87 Å, in addition to contributions from non-specific dispersion interactions (which would favor a planar structure). [43] These competing interactions lead to BDA adsorption at an angle of 10.3° with the Au surface. Monomers at different coverages bind in similar configurations. The only exception is the monomer on a $3a_1 \times 3a_2$ slab. At this high coverage, due to the strong dipole-dipole repulsion between adsorbates, Au-N bonds are unable to form, and the adsorbate is bound to the substrate by dispersion forces alone. As a result, the distance between the N atom and the underlying Au atom is elongated to 3.28 Å and the molecule-substrate angle decreases to 5.4°.

In Fig. 1b), we show BDA in the self-assembled linear chain structure of the BDA, which is constructed following experiments. The molecules are oriented along the [112] direction, but they are now in a *cis*-configuration to facilitate the formation of the N-H…N hydrogen bonds (of 2.25 Å) between neighboring molecules. As in the monomer phase, the molecules in the linear

chains also bind preferentially to a single Au atom but with a slightly shorter N-Au bond of 2.82 Å and a molecule-substrate angle of 16.6°, consistent with the experimental value of 24°±10° [18]. The optimized geometries of the linear chains are unchanged as a function of coverage and inter-chain spacing, as shown in the SM [36]. We note that a similar linear chain structure of BDA on Au(111) was proposed in prior theoretical work. [42] The structure in Ref [42] differs from our geometry in that the BDA molecules are proposed to be in the *trans*-conformation, which leads to a larger predicted angle of 21° with the Au surface. Our calculations indicate that the *trans*-conformation is less stable than the *cis* by 0.11 eV/molecule due to the absence of intermolecular hydrogen bonds. Therefore, we adopt the *cis* linear chain shown in Fig. 1 b) for all subsequent calculations.

Fig 2 a) shows the calculated adsorption energy E_{ad} for each coverage (defined in the SM [36]) as a function of A. For the linear structure, E_{ad} monotonically decreases as A increases; while for the monomeric phase, the $E_{ad}(A)$ curve shows a similar trend, but a small feature appears at A=3.69 nm^2, corresponding to the $7a_1 \times 7a_2$ supercell. As discussed in the SM [36], this tiny feature is a result of a slight buckling of the BDA adsorbate occuring as a function of coverage (leading to small changes in adsorption energy of about 0.05 eV, e.g. for A=3.69 nm^2). Importantly, Fig. 2a) shows that the E_{ad} of the linear chains are always lower than those of the monomers, indicating that the linear chains are energetically favored at all the coverages considered, consistent with the observations of Ref. [21]. We note that similar chain-like assemblies have been observed for styrene on Si [44].

Having established the structural energetics of the two BDA phases, we now turn to a comparison of their calculated electronic structure. We first calculate the differences in Au(111) work functions (ϕ) of BDA monomer and linear chain adsorbate phases. As is standard, we compute ϕ as the difference between the vacuum potential and the system Fermi energy (as shown in Fig. S3). We compute ϕ for Au(111) to be 5.55 eV, in good agreement with

experimental values and prior calculations. [45] Values of ϕ for BDA-covered Au(111), as shown in Fig. 2b), are all smaller than that of bare Au(111), implying the total effective dipole moments of both BDA adsorbate phases, including both intrinsic and binding-induced contributions, point toward the Au surface [46]. Furthermore, we find that the ϕ values associated with the linear chain structures are always smaller than those associated with the monomer phase, with differences up to 0.9 eV at high coverage ($A \approx 0.8$ nm^2). This result indicates that the effective dipole moments of BDA in the linear chain structures are significantly larger in magnitude than those of the BDA monomer phase.

The alignment of the BDA HOMO resonance energies, relative to E_F, for the two phases is also considerably different, as we show via direct calculation of the DFT projected densities of states (PDOS). In the BDA PDOS shown in black in Fig. 3, the HOMO resonances are identified via the projection of the wave functions of the associated isolated BDA adsorbate phase onto those of the combined BDA-Au system (as shown in Fig. S4). That is, for both the monomer and linear chain phases at a particular coverages, we remove the Au surface atoms from the relaxed supercell, recompute the ground state energy and density with the BDA atoms fixed, and calculate the HOMO of this "freestanding" BDA molecule or chain at the Γ point. We then project this HOMO onto all eigenstates of the adsorbate-Au system at Γ, and weight the DOS with this projection to identify the HOMO resonances of the adsorbate. The HOMO resonances corresponding to both phases at high coverage are shaded in blue in Fig. 3. The HOMO energies of adsorbed BDA in the monomer phase are broadened due to the molecule-substrate hybridization. In the linear chain phase, the PDOS is further broadened by the intermolecular hydrogen bonds, and moreover the linear chain HOMO resonances are deeper, relative to E_F, than for the monomer phase, consistent with the calculated trend in workfunctions and effective induced adsorbate dipoles.

Due to the limitations of Kohn-Sham DFT for describing quasiparticle states, [47] the

calculated DFT-PBE HOMO resonance energies ($E_{HOMO,DFT}$) are underestimated, as is well known [6,18,19,48]. To include exchange and correlation effects missing from DFT orbital energies, we correct the $E_{HOMO,DFT}$ values via the DFT+Σ method, a model GW approach first established for BDA-Au junctions but extended to adsorbates on surfaces. [6] Using this method, the quasiparticle energy associated with the HOMO of adsorbed BDA is calculated as

$$E_{HOMO,QP} = E_{HOMO,DFT} + \Delta\Sigma_{mol} + P, (2)$$

where the last two terms on the right hand side, $\Delta\Sigma_{mol}$ and P, comprise the model GW corrections, and we define and further elaborate on these terms below.

In Eq. (2), $\Delta\Sigma_{mol}$ is the self-energy correction for the HOMO energy of a freestanding molecule, obtained here from G_0W_0 calculations. For a gas-phase BDA molecule, we consider an isolated molecule and compute $\Delta\Sigma_{mol}$ = -2.67 eV, leading to a correction of the PBE Kohn-Sham HOMO energy, relative to vacuum, from -4.55 eV to -7.22 eV, in good agreement with the measured gas-phase ionization potential of -7.34 eV. [49,50] For the freestanding adsorbates, $\Delta\Sigma_{mol}$ is determined by including nonlocal polarization effects from neighboring molecules: for these systems, our G_0W_0 calculations are performed with periodic boundary conditions without a Coulomb truncation (and therefore include nonlocal interchain polarization effects). The obtained values of $\Delta\Sigma_{mol}$ for the $a_1' \times a_2'$ chain phase and for the $3a_1 \times 3a_2$, $4a_1 \times 4a_2$, and $5a_1 \times 5a_2$ monomer phases are -2.38 eV, -2.49 eV, -2.55 eV, and -2.58 eV, respectively. For the linear chain phase, $\Delta\Sigma_{mol}$ is reduced relative to the gas-phase, but increases towards the gas-phase value as A increases; these differences and their trends are a direct consequence of nonlocal polarization from neighboring molecules.

In Eq. (2), P is the nonlocal polarization associated with the metallic Au substrate. Creation of a quasi-hole in any of the adsorbate BDA phases considered here induces additional substrate polarization, screening the quasi-hole and raising the HOMO energy relative to E_F. Following previous work [6,7], to quantify the magnitude of this polarization, we treat the quasi-

hole approximately, as a point charge located at the geometrical center of the molecule; we estimate P via a simple image potential model [6] as

$$P = e^2/4|z\text{-}z_0|. \quad (3)$$

In this equation, z is the position of the geometrical center of the adsorbed BDA molecule normal to the surface, and z_0 is the image plane position, which we have taken to be 1.47 Å above the outer atomic plane of the Au surface, following the classical approach of Ref. [19,51]. For the $a_1'\times a_2'$ chain phase, and for the $3a_1\times 3a_2$, $4a_1\times 4a_2$, and $5a_1\times 5a_2$ monomer phases, the z values used here are 3.66 Å, 3.48 Å, 3.37 Å, and 3.36 Å, respectively; for each $|z\text{-}z_0|$, the corresponding P values, via Eq.(3), are 1.64 eV, 1.80 eV, 1.90 eV, and 1.91 eV, respectively. In the linear chain phases, the large molecule-surface angle considerably lifts the geometrical centers of BDA from the surface, increasing $|z\text{-}z_0|$ and significantly reducing P.

Using the above values of $\Delta\Sigma_{mol}$ and P, we approximately correct the DFT HOMO resonances of BDA adsorbates by rigidly shifting the corresponding PDOS peaks, and neglecting any changes in the coupling of the molecular orbitals to the continuum states of Au that affect the shapes of the PDOS peaks. The corrected HOMO resonances are shown in Fig. 3 shaded in red. We find that all DFT+Σ HOMO resonances are significantly closer to the experimental results obtained with UPS and XPS, [18] shaded in grey and yellow in Fig. 3. However, only the HOMO resonance of the chain phase lies within the window of the experimental values. Furthermore, we find that the cumulative effects of the polarization – from both the substrate and neighboring molecules – on the HOMO resonances of the monomer and linear chain structures are similar. We can therefore conclude that the differences in HOMO resonance energies are dominated by differences in induced interface dipoles for the monomer and linear chain phases. Moreover, as analyzed in the SM [36], the effect of coverage on the HOMO resonance of the chain phase is negligible; resulting in only small variations of the HOMO resonance energy, less than ±0.1 eV.

We note that, in a previous calculation using the same method (DFT+Σ) with a different

geometry, [18] the HOMO energy of a BDA monomer on Au(111) was found to be -1.6 eV relative to the Fermi level, lower than our monomer results but consistent with the experimental values. However, in Ref. [18], the angle between the adsorbed molecule and the Au surface was fixed at the value of 24° determined by near edge X-ray adsorption fine structure measurements [18], which, although not stable for the monomer in our fully-relaxed DFT calculations with vdW-DF2, is actually close to the angle we obtain for the linear chain structure here. Moreover, we note that a recent calculation [13] using a new nonclassical approach resulted in an image plane closer to the Au surface; this would lead to the prediction of a lightly deeper resonance relative to E_{F} for the chain phase, still within the experimental error bars.

In summary, using DFT with van der Waals density functionals, we have investigated a new linear chain phase of BDA molecules on Au(111). We found that this structure is formed via intermolecular hydrogen bonds, and it is energetically more stable than a BDA adsorbate monomer phase. Furthermore, we have calculated the energy level alignment at BDA-Au interfaces with model self-energy corrections including information from GW calculations and, in an approximate fashion, nonocal polarization effects from the substrate and the neighboring molecules. Our results show that, in the linear chain phase, because of the larger induced interface dipole, the BDA HOMO resonance energy relative to the Fermi energy of the Au substrate is remarkably lower than those found for monomers and agrees well with the experimental values obtained with XPS and UPS. These findings emphasize the important role of the geometries of molecular adsorbates in determining the energy level alignment at organic-inorganic interfaces.

References:

[1] S. V. Aradhya and L. Venkataraman, Nat. Nanotechnol. 8, 399 (2013).

[2] K. Moth-Poulsen and T. Bj_rnholm, Nat. Nanotechnol. 4, 551 (2009).

[3] S. R. Forrest, Nature 428, 911 (2004).

[4] C. Joachim, J. Gimzewski, and A. Aviram, Nature 408, 541 (2000).

[5] G. Heimel, L. Romaner, J.-L. Bredas, and E. Zojer, Phys. Rev. Lett. 96, 196806 (2006).

[6] J. B. Neaton, M. S. Hybertsen, and S. G. Louie, Phys. Rev. Lett. 97, 216405 (2006).

[7] S. Y. Quek, L. Venkataraman, H. J. Choi, S. G. Louie, M. S. Hybertsen, and J. Neaton, Nano Lett. 7, 3477 (2007).

[8] Y. Zhan, M. De Jong, F. Li, V. Dediu, M. Fahlman, and W. R. Salaneck, Phys. Rev. B 78, 045208 (2008).

[9] X. Liu, Y. Zhan, S. Braun, F. Li, and M. Fahlman, Phys. Rev. B 80, 115401 (2009).

[10] S. Y. Sayed, J. A. Fereiro, H. Yan, R. L. McCreery, and A. J. Bergren, Proc. Natl. Acad. Sci. 109, 11498 (2012).

[11] L. Ley, Y. Smets, C. I. Pakes, and J. Ristein, Adv. Funct. Mater. 23, 794 (2013).

[12] M. L. Perrin, C. J. Verzijl, C. A. Martin, A. J. Shaikh, R. Eelkema, J. H. van Esch, J. M. van Ruitenbeek, J. M. Thijssen, H. S. van der Zant, and D. Dulic, Nature nanotech. 8, 282 (2013).

[13] D. A. Egger, Z.-F. Liu, J. B. Neaton, and L. Kronik, Nano Lett. 15, 2448 (2015).

[14] L. Venkataraman, J. E. Klare, C. Nuckolls, M. S. Hybertsen, and M. L. Steigerwald, Nature 442, 904 (2006).

[15] L. Venkataraman, J. E. Klare, I. W. Tam, C. Nuckolls, M. S. Hybertsen, and M. L. Steigerwald, Nano Lett. 6, 458 (2006).

[16] S. Y. Quek, H. J. Choi, S. G. Louie, and J. B. Neaton, Nano Lett. 9, 3949 (2009).

[17] T. Kim, P. Darancet, J. R. Widawsky, M. Kotiuga, S. Y. Quek, J. B. Neaton, and L. Venkataraman, Nano Lett. 14, 794 (2014).

[18] M. DellAngela, G. Kladnik, A. Cossaro, A. Verdini, M. Kamenetska, I. Tamblyn, S. Quek, J. Neaton, D. Cvetko, A. Morgante, et al., Nano Lett. 10, 2470 (2010).

[19] I. Tamblyn, P. Darancet, S. Y. Quek, S. A. Bonev, and J. B. Neaton, Phys. Rev. B 84, 201402 (2011).

[20] A. Biller, I. Tamblyn, J. B. Neaton, and L. Kronik, J. Chem. Phys. 135, 164706 (2011).

[21] T. K. Haxton, H. Zhou, I. Tamblyn, D. Eom, Z. Hu, J. B. Neaton, T. F. Heinz, and S. Whitelam, Phys. Rev. Lett. 111, 265701 (2013).

[22] G. Kresse and J. Hafner, Phys. Rev. B 47, 558 (1993).

[23] G. Kresse and J. Hafner, Phys. Rev. B 49, 14251 (1994).

[24] G. Kresse and J. Furthmller, Comput. Mat. Sci. 6, 15 (1996).

[25] G. Kresse and J. Furthmller, Phys. Rev. B 54, 11169 (1996).

[26] J. P. Perdew, K. Burke, and M. Ernzerhof, Phys. Rev. Lett. 77, 3865 (1996).

[27] J. P. Perdew, K. Burke, and M. Ernzerhof, Phys. Rev. Lett. 78, 1396 (1997).

[28] T. Thonhauser, V. R. Cooper, S. Li, A. Puzder, P. Hyldgaard, and D. C. Langreth, Phys. Rev. B 76, 125112 (2007).

[29] M. Dion, H. Rydberg, E. Schröder, D. C. Langreth, and B. I. Lundqvist, Phys. Rev. Lett. 92, 246401 (2004).

[30] G. Román-Pérez and J. M. Soler, Phys. Rev. Lett. 103, 096102 (2009).

[31] K. Lee, E. D. Murray, L. Kong, B. I. Lundqvist, and D. C. Langreth, Phys. Rev. B 82, 081101 (2010).

[32] J. Klimes, D. R. Bowler, and A. Michaelides, Phys. Rev. B 83, 195131 (2011).

[33] P. E. Blchl, Phys. Rev. B 50, 17953 (1994).

[34] G. Kresse and D. Joubert, Phys. Rev. B 59, 1758 (1999).

[35] P. Haas, F. Tran, and P. Blaha, Phys. Rev. B 79, 085104 (2009).

[36] See Supplemental Material at [URL] for computational details and complementary calculation results.

[37] J. Neugebauer and M. Scheffer, Phys. Rev. B 46, 16067 (1992).

[38] G. Makov and M. Payne, Phys. Rev. B 51, 4014 (1995).

[39] J. Deslippe, G. Samsonidze, D. A. Strubbe, M. Jain, M. L. Cohen, and S. G. Louie, Comput. Phys. Commun. 183, 1269 (2012).

[40] S. Sharifzadeh, I. Tamblyn, P. Doak, P.T. Darancet, and J.B. Neaton, Eur. Phys. J. B, 85, 323 (2012)

[41] X. Gonze, B. Amadon, P.-M. Anglade, J. -M. Beuken, F. Bottin, P. Boulanger, F. Bruneval et al. Comput. Phys. Commun. 180, 2582 (2009).

[42] D. Le, M. Aminpour, A. Kiejna, and T. S. Rahman, J. Phys.: Condens. Matter. 24, 222001 (2012).

[43] G. Li, I. Tamblyn, V. R. Cooper, H.-J. Gao, and J. B. Neaton, Phys. Rev. B 85, 121409 (2012).

[44] G. Li, V. R. Cooper, J.-H. Cho, S. Du, H.-J. Gao, and Z. Zhang, Phys. Rev. B 84, 241406 (2011).

[45] C. Fall, N. Binggeli, and A. Baldereschi, Phys. Rev. B 61, 8489 (2000).

[46] J. B. Rivest, G. Li, I. D. Sharp, J. B. Neaton, and D. J. Milliron, J. Phys. Chem. Lett. 5, 2450 (2014)

[47] R. O. Jones and O. Gunnarsson, Rev. Mod. Phys. 61, 689 (1989).

[48] T. Rangel, A. Ferretti, P. E. Trevisanutto, V. Olevano, and G.-M. Rignanese, Phys. Rev. B 84, 045426 (2011)

[49] D. Streets, W. Elane Hall, and G. P. Ceasar, Chem. Phys. Lett. 17, 90 (1972).

[50] D. E. Cabelli, A. H. Cowley, and M. J. Dewar, J. Am. Chem. Soc. 103, 3286 (1981).

[51] S. Lam and R. Needs, J. Phys.: Condens. Matter. 5, 2101 (1993).

FIG. 1: The a) side view and b) top view of a BDA monomer in a $4a_1 \times 4a_2$ supercell; the c) side view and d) top view of the linear structure of BDA on Au(111). The black solid lines in a) and c) indicate the in-plane unit cells. The black arrows indicate the primitive lattice vectors (a_1 and a_2) of Au(111). The Au, C, H and N atoms are in golden, green, white, and blue, respectively.
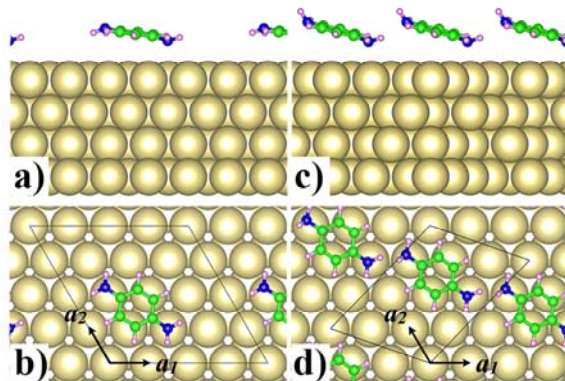
FIG. 2: The a) adsorption energies and b) work functions as a function of the surface area per BDA adsorbate (A). The monomeric phase and the linear structure are in blue and red, respectively.
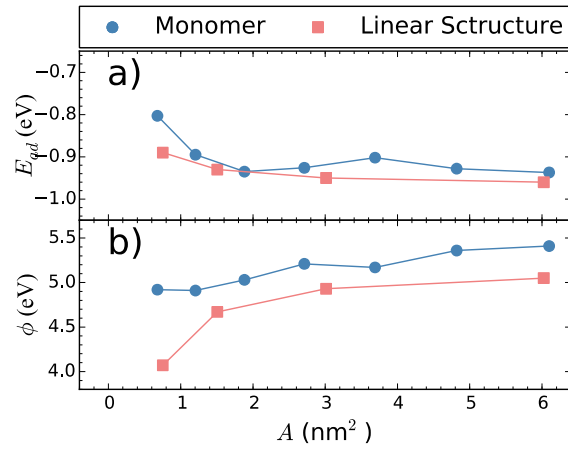
FIG. 3: The HOMO resonances of BDA adsorbates relative to the Au Fermi level. The DFT PDOS of the BDA adsorbates are plotted as the solid black curves, and the HOMO resonances are marked with blue shades. The HOMO resonances corrected with DFT+$\Delta\Sigma$ and the experimental results obtained via UPS and XPS are shown as the red, grey, and yellow shdes, respectively. The black dash lines indicate the Fermi level of Au. The panels are marked with the sizes of the corresponding supercells.